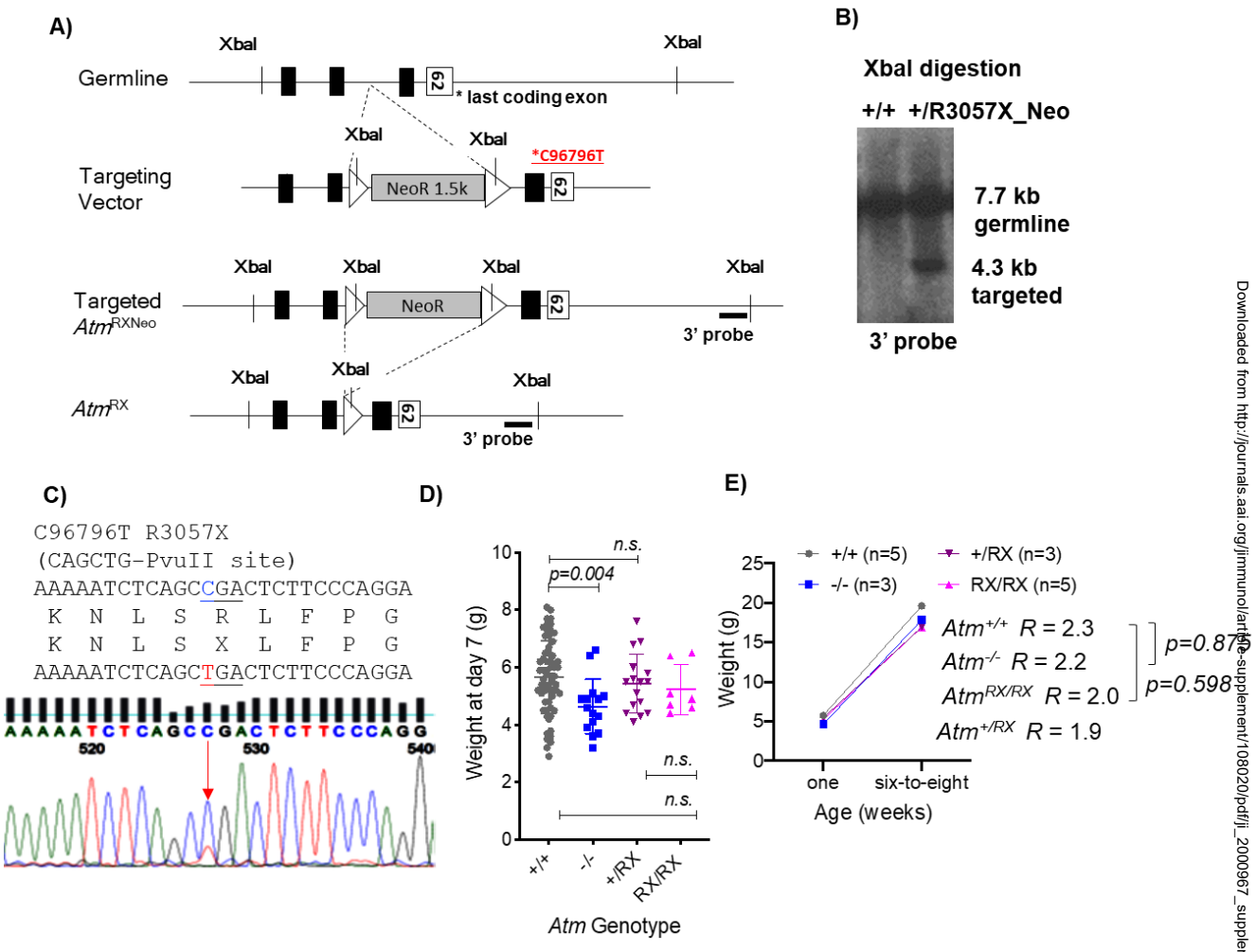

Fig S1. Diagram of the *Atm*^{R3057X} (*Atm*$^{RX/RX}$) mouse targeting strategy

A) The targeting scheme of the *Atm*^{R3057X} allele. The diagram shows the germline (top), targeting vector (second row), and targeted allele (*Atm*^{RNeo} – for NeoR positive), and the final neo-deleted mutant *Atm*^{RX} allele (bottom). The open triangles represent the FRT sites and solid boxes represent exons. The exon containing the C96796T mutation is the last coding exon of the *Atm* gene and is marked as an open box. The restriction enzymes are marked as XbaI; Kp, KpnI; H3, HindIII; B, BglII. The map is not drawn to scale. **B)** Representative Southern blotting analysis with XbaI digested DNA from control and targeted (+/R3057X-NeoR) ES cells. The Germline band is 7.7 kb and the targeted band is 4.3 kb. **C)** The Sanger sequencing result of the targeted clones. Please note the chromatogram was read on the complementary strand (non-template strand of Atm). **D)** The weight (gram) of 7-day old *Atm*$^{+/+}$, *Atm*$^{-/-}$, *Atm*$^{+/RX}$, and *Atm*$^{RX/RX}$ mice (n>=12 for each genotype). On the graph, horizontal lines represent mean ± standard deviation. P-values were calculated using unpaired two-tailed Student's t-test. **E)** Mouse body weight measured sequentially at one week and six-to-eight weeks of age (n>=3 for each genotype). The gram weight gain per week (R) is marked on the figure. The p-values were calculated via unpaired two-tailed Student's t-test.

A) Thymus

x10⁶	n	Total	DP	CD4⁺ SP	CD8⁺ SP
Atm$^{+/+}$	5	89.9 ± 24.2	64.2 ± 17.8	12.7 ± 4.0	3.9 ± 1.4
Atm$^{-/-}$	3	68.6 ± 1.6	66.3 ± 23.5	6.1 ± 2.3	2.2 ± 0.8
Atm$^{RX/RX}$	6	94.3 ± 3.8	75.5 ± 30.6	7.4 ± 3.1	2.2 ± 0.8

B)

%	n	Total	DP	CD4⁺ SP	CD8⁺ SP
Atm$^{+/+}$	5	90.6 ± 0.9	70.8 ± 2.1	13.9 ± 1.4	4.4 ± 0.7
Atm$^{-/-}$	3	88.1 ± 6.6	78.1 ± 1.3	6.7 ± 0.8	2.4 ± 0.4
Atm$^{RX/RX}$	6	84.7 ± 1.8	79.9 ± 2.1	7.2 ± 0.6	2.3 ± 0.3

C)

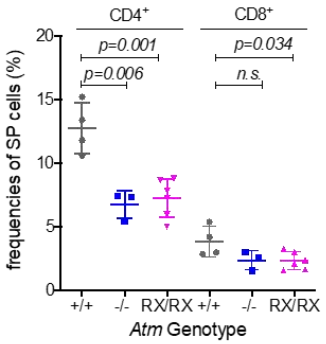

D) Bone Marrow

%	n	B220⁺CD43⁺ (proB)	B220⁺IgM⁻ (proB + preB)	PreB/ProB ratio	B220⁺IgM^{mid} (naive)	B220^{high}IgM^{high} (re-circulating)
Atm$^{+/+}$	3	4.1 ± 1.1	8.1 ± 1.3	1.2 ± 1.1	5.8 ± 1.5	2.0 ± 0.6
Atm$^{-/-}$	2	4.8 ± 1.2	7.0 ± 1.7	0.4 ± 0.01	6.4 ± 1.3	2.3 ± 0.3
Atm$^{RX/RX}$	4	5.2 ± 0.8	9.9 ± 1.3	1.1 ± 0.4	5.9 ± 1.2	1.9 ± 0.5

Spleen

x10⁶	n	Total	B220^{high}IgM^{high}
Atm$^{+/+}$	5	37.1 ± 13.6	14.3 ± 2.0
Atm$^{-/-}$	3	8.7 ± 1.1	2.0 ± 0.5
Atm$^{RX/RX}$	6	26.9 ± 15.0	11.09 ± 8.1

E) Bone Marrow at 5-6 week **F)** Bone Marrow at 25-26 week **G)**

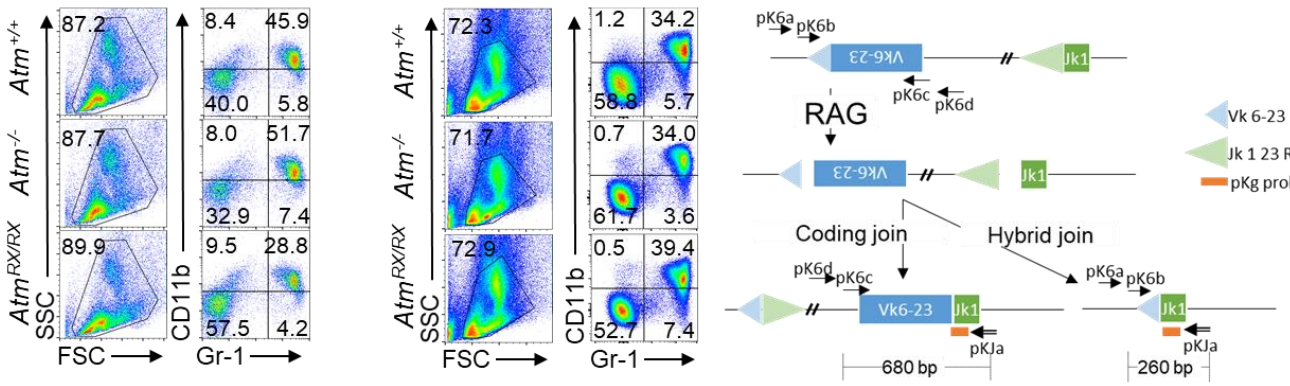

Fig S2. Immature B cell and myeloid development is largely unaffected in *Atm*$^{RX/RX}$ mice

A) The table summarizes T cell development (by absolute cell number) in the thymus. The numbers indicate the mean T cell counts ± standard error (n>= 3). **B)** The table summarizes T cell development (by relative frequency) in the thymus. The numbers indicate the mean ± standard error (n>= 3) and represent the percentages of cell populations detected by FACS analysis. **C)** The frequency (%) of CD4+ and CD8+ single-positive cells in the thymus from 4-6-week-old *Atm*$^{+/+}$, *Atm*$^{-/-}$ and *Atm*$^{RX/RX}$ mice. Horizontal lines on the graph represent mean ± standard deviation. P-values were calculated using unpaired two-tailed Student's t-test. **D)** The table summarizes B cell development in the bone marrow. The numbers represent the percentages of different B cell populations indicated as the mean ± standard error (n>= 2). The table below represents the mean ± standard error of total splenocytes and splenic B cells from *Atm*$^{+/+}$, *Atm* $^{-/-}$ and *Atm*$^{RX/RX}$ mice. **E) and F)** Representative flow cytometry analyses of the myeloid cell population in bone marrow from *Atm*$^{+/+}$, *Atm*$^{-/-}$ and *Atm*$^{R/R}$ mice of various ages. The percentage of cells in each quadrant is marked on the plots. **G)** Diagram of the coding joints (CJ) and hybrid joints (HJ) involving Vκ6-23 at the Ig κ locus.

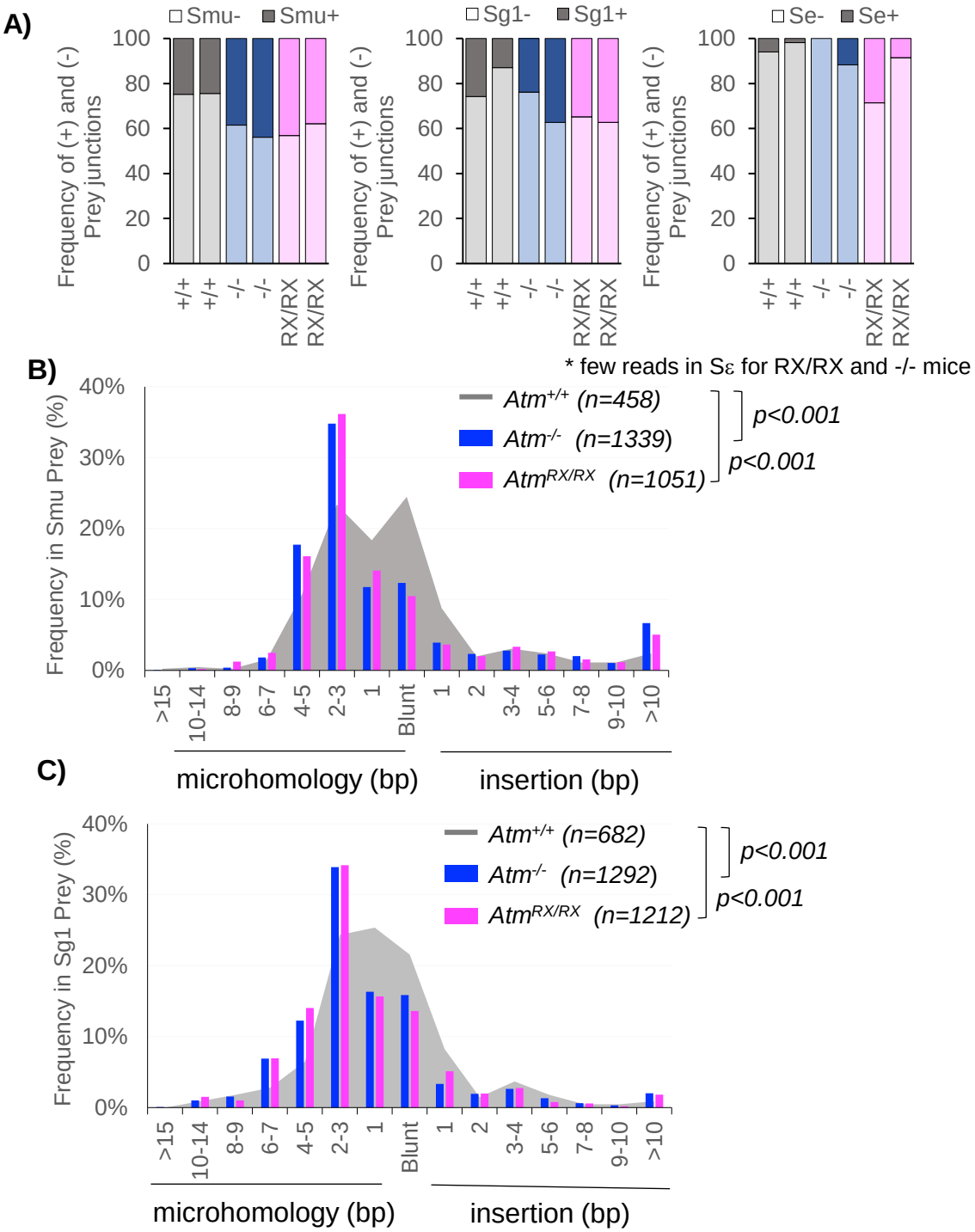

Fig S3. HTGTS analysis of stimulated *Atm*$^{RX/RX}$ B lymphocytes

A) The relative frequencies of (-) strand/deletional and (+) strand/inversional prey sites detected within Sμ (left), Sγ1(middle) and Sε switch region. Deletional (-) and inversional (+) break sites are normalized to the total number of Sμ, Sγ1, or Sε prey break sites respectively. Bars represent data from two independent libraries per genotype. **B)** The distribution of Sμ junctions by junction type. The graph represents the pooled Sμ junctions from two independent libraries of each genotype. P-values were calculated using the Kolmogorov–Smirnov test. **C)** The distribution of Sγ1 joint by MH and INS length. The graph represents the pooled Sγ1 joint from two libraries prepared from two independent mice of each genotype. P-values were calculated using the Kolmogorov–Smirnov test.

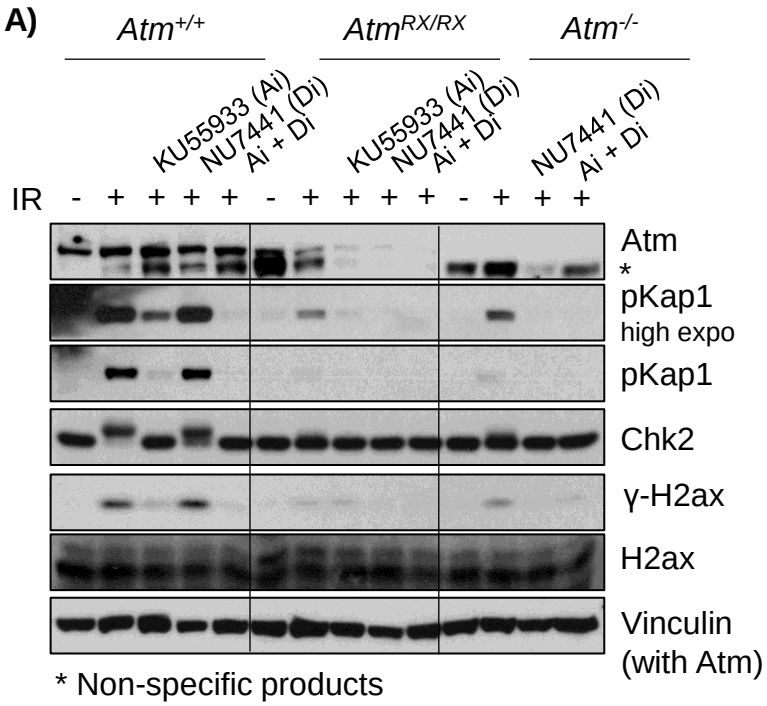

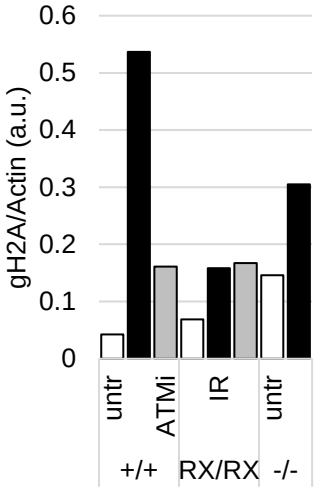

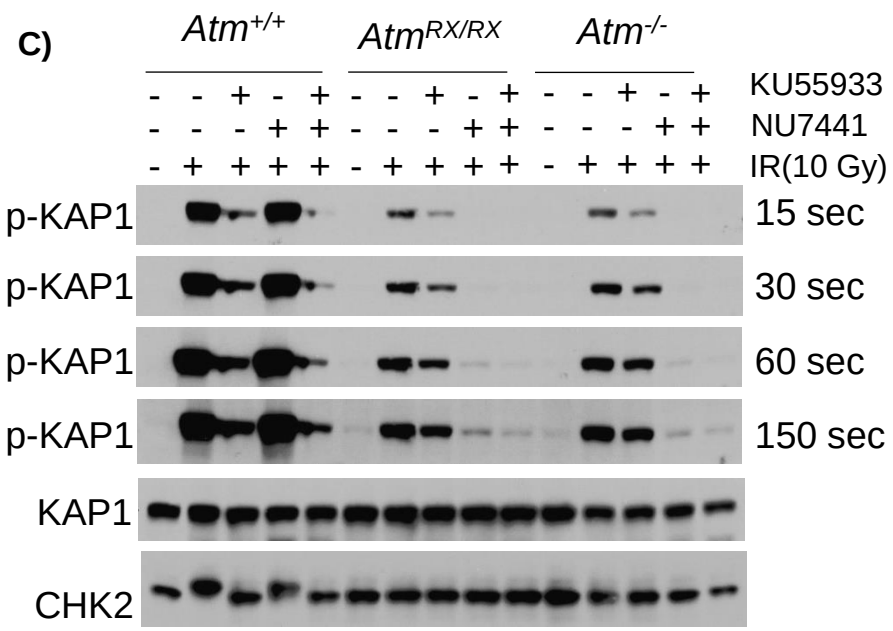

Fig S4. Residual Atm-RX protein might be activated by DSBs

A) Immunoblot analysis of *Atm*$^{+/+}$, *Atm*$^{RX/RX}$, and *Atm*$^{-/-}$ Abelson-transformed B cells 2 hours after irradiation with 15 Gy dose, left untreated or treated with ATM inhibitor Ku55933 (15 μM), DNA-PK inhibitor Nu7441(15μM) or both. **B)** The quantification of the gH2AX/actin intensity before and after IR (from panel A). **C)** Independent immunoblot analysis of *Atm*$^{+/+}$, *Atm*$^{RX/RX}$, and *Atm*$^{-/-}$ Abelson-transformed B cells 2 hours after irradiation with 10 Gy dose, left untreated or treated with ATM inhibitor Ku55933 (15 μM), DNA-PK inhibitor Nu7441(15μM) or both. Different exposure time of pKAP1 was shown. At lower exposure, ATM inhibitor (Ku55933) used at 15 μM suppresses IR induced Kap1 phosphorylation even in *Atm*$^{-/-}$ cells, likely by suppressing the related DNA-PK. This difference is less obvious at long exposure when the signals are saturated. The 30s exposure was used for the quantification on Figure 6D.

pκJa	GGAGAGTGCCAGAATCTGGTTTCAG
pκ6a	TGCATGTCAGAGGGCACAACTG
pκ6b	CTACCAAACTTTGCAACACACAGGC
pκ6c	ACATGTTGCTGTGGTTGTCTGGTG
pκ6d	GACCAGCATGGGCATCAAGATGGAGAC
pκg1	AAGCTGGAAATCAAACGTAAGTAG
pβa	GCATTCATATCACACAGTGAGCACC
pβb	GGGGTGTACCATAAAGGGGAAATCA
pβc	GCAGTTAGGTTATCAGAGGAGGGCA
pβd	TGGCCAGGTAGAGTCGGTGG
pβe	TGAGAGCTGTCTCCTACTATCGAT
pβf	AGAGTCGGTGGTGCAACTGAACCT
pβg	TGAGAAGCAGCTTCTCCGTG
IMR042	CTAGGCCACAGAATTGAAAGATCT
IMR043	GTAGGTGGAAATTCTAGCATGATGC
IMR042-2	GGTGTTGCTTTATTTGCTAATCTGG

Fig S5. The list of PCR primers used to measure Vκ6-23 and TCRβ hybrid joint formation.